Journal of The Electrochemical Society, **148** (7) A768-A774 (2001)
0013-4651/2001/148(7)/A768/7/$7.00 © The Electrochemical Society, Inc.

Evidence for Reversible Formation of Metallic Cu in $Cu_{0.1}V_2O_5$ Xerogel Cathodes during Intercalation Cycling of Li^+ Ions as Detected by X-Ray Absorption Spectroscopy

Marco Giorgetti,[a,*,e] Sanjeev Mukerjee,[b,] Stefano Passerini,[c,**] James McBreen,[d,**] and William H. Smyrl[a,***,z]**

[a]*Corrosion Research Center, Department of Chemical Engineering and Materials Science, University of Minnesota, Minneapolis, Minnesota 55455, USA*
[b]*Department of Chemistry, Northeastern University, Boston, Massachusetts 02115, USA*
[c]*ENEA, C.R. Casaccia, Rome 00060, Italy*
[d]*Department of Applied Science, Material Science Division, Brookhaven National Laboratory, Upton, New York 11973, USA*

Vanadium pentoxide materials prepared through sol-gel processes (xerogel, aerogel, and aerogel-like) act as excellent intercalation hosts for lithium as well as polyvalent cations. The large lithium insertion capacity of these materials makes them attractive for use as cathodes in high-capacity lithium batteries. Copper-doped V_2O_5-based cathodes have excellent properties in terms of high intercalation rate and very good reversibility upon cycling with no capacity fading after more than 450 cycles. This paper reports *in situ* X-ray absorption spectroscopy (XAS) investigations of copper-doped V_2O_5 xerogel. The K-edge X-ray absorption thresholds of V and Cu were studied. The local structure around copper is found to change dramatically during individual insertion/release cycles for Li^+ ions. The XAS analysis indicates that the lithiation of the $Cu_{0.1}V_2O_5$ xerogel cathode proceeds with concurrent formation of copper metal. However, the starting compound is regenerated upon releasing the inserted lithium (charging the cathode), thus revealing the foundation for excellent structural and electronic reversibility of the material.
 [DOI: 10.1149/1.1379029]

Manuscript submitted July 17, 2000; revised manuscript received March 20, 2001. Available electronically June 8, 2001.

Many vanadium pentoxide gels have been synthesized during the last two decades via facile sol-gel chemistry[1] or hydrothermal methods.[2] A common characteristic of the materials is the layered structure that may accommodate various chemical species. The materials serve as hosts into which guests are inserted and, successively and reversibly, released. The rate at which such reactions takes place in these materials and the associated change of Gibbs free energy are of fundamental importance because they permit the use of the materials in intercalation batteries.

Our research group at the University of Minnesota is involved in the development of gel-based V_2O_5 compounds as cathodes for lithium batteries. Previous results indicated that large lithium insertion capacities can be achieved in several vanadium oxide gel materials.[3-5] By using composite structures of V_2O_5 xerogel material (XRG), lithium cells have been successfully studied with liquid and polymer electrolytes.[5,6] The characterization of the intercalation properties of V_2O_5 aerogels (ARG) has been extended to polyvalent cations such as Al^{3+}, Zn^{2+}, and Mg^{2+}, therein showing the versatility of the host.[7] The electrochemical performance of (aerogel-like) V_2O_5 synthesized under subcritical conditions has also been reported.[8]

In recent work, it was found that vanadium oxide could be easily doped with a metal in the hydrogel form by a simple reaction with a known amount of the doping metal (copper, silver, zinc, nickel, and aluminum). The characterization of gel-based, copper-doped V_2O_5 materials has been reported earlier.[9,10] The materials maintain the layered structure typical of V_2O_5 but with enhanced performance. Cathodes based on these materials have a potential of around 3.7 V (*vs.* Li) in the pristine state and are able to reversibly intercalate a large number of lithium ions ($x > 2$). This leads to experimental specific capacities exceeding 300 mAh/g at the C/100 rate and specific energies exceeding 750 Wh/kg.[9] Cyclic voltammetry and galvanostatic insertion of doped V_2O_5 materials indicate the possible reduction of the doping ion (silver or copper) to the metallic state during lithium insertion.

In the present contribution, we focus on the effects produced by lithium insertion in copper-doped V_2O_5 XRG cathodes by using *in situ* X-ray absorption spectroscopy (XAS) as a local structural tool. The technique is sensitive to short-range order (a few angstroms around the selected atom) and can be applied to disordered, amorphous, and crystalline materials. Previous reports based on *in situ* XAS studies have given details on various topics including electrochemical interfaces,[11] electrode surface,[12,13] Pt/C catalysts,[14] batteries,[15] and biology.[16] In our application, the vanadium and the copper local structural arrangement could be monitored during the intercalation process, revealing the modification that occurred upon lithium insertion and release.

Previous studies by the XAS technique on the V_2O_5-based compounds have allowed us to determine fundamental structural information on a wide variety of native and intercalated V_2O_5 compounds.[17-23] In particular, a study based on polarized XAS measurements[22] on the native XRG has definitively demonstrated that V_2O_5 XRG compound has a bilayer structure. Also, the characterization of a zinc-intercalated V_2O_5 ARG has shown[18] a new and unconventional site for the guest ion. The Zn^{2+} ions are located within a single V_2O_5 layer, leaving the interlayer space available for further ion insertion.[18] Further, *in situ* extended X-ray absorption fine structure (EXAFS) and X-ray absorption near-edge structure (XANES) results on the V_2O_5 XRG cathode[21] have demonstrated that the amorphous nature of the material allows for facile lattice expansions and contractions upon lithium intercalation without any major disruption of the V_2O_5 layer structure.

In this work, we show that the analysis of the Cu K-edge spectra indicates that metallic Cu is formed concurrently upon the lithium insertion. However, upon removal of lithium ions the Cu metal formed is oxidized again and reinserted into its original site. There is no loss of Cu^{+2} ions to the electrolyte. The results demonstrate the complete structural and electronic reversibility of the cathodic material investigated.

* Electrochemical Society Student Member.
** Electrochemical Society Active Member.
*** Electrochemical Society Fellow.
[e] Present address: Department of Physical and Inorganic Chemistry, University of Bologna, Bologna 40136, Italy.
[z] E-mail: smyrl001@maroon.tc.umn.edu

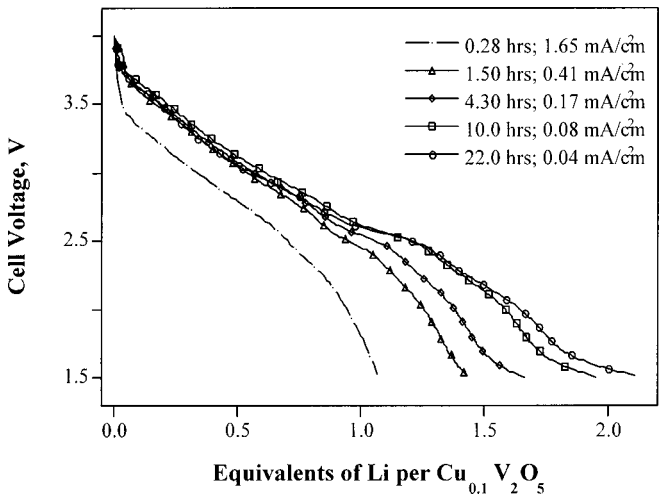

Figure 1. Typical discharge behavior of spray-coated $Cu_{0.1}V_2O_5$ electrodes in coin cell assembly with 1 M $LiClO_4$-PC as electrolyte and lithium anode at room temperature. The discharge current and time are indicated in the legend.

Experimental

Synthesis.—Vanadium pentoxide hydrogels were synthesized by an ion-exchange process with sodium metavanadate.[1,6] The copper-doped V_2O_5 was prepared as described earlier by Coustier *et al.*[10] Briefly, the doping was performed by mixing the selected stoichiometric amount of copper powder (Alfa 99.997% purity) with the V_2O_5 hydrogel. X-ray diffraction (XRD) spectra were taken on the dry, doped material in order to verify the completion of the reaction, *i.e.*, no peaks associated with metallic copper were found.

Electrochemical tests.—$Cu_{0.1}V_2O_5$ xerogel electrodes were prepared by spray coating a mixture of the active material with carbon (Ketjen black, Akzonobel) and binder (Kynar, ELF-Atochem) in cyclopentanone (Fluka), onto 25 μm thick aluminum foils. The final weight ratio of the three components in the dry cathode was 80:10:10, respectively. The active material mass loading ranged from 3 to 4 mg cm^{-2}.

The electrochemical tests were performed in a classical button cell where a lithium disk was used as the negative electrode and the electrolyte was 1 M $LiClO_4$ in propylene carbonate (PC) supported on porous polypropylene (Celgard). The lithium intercalation-deintercalation reaction was driven by an Arbin battery cycler.

XAS experiments.—To perform *in situ* XAS measurements, $Cu_{0.1}V_2O_5$ xerogel cathodes were placed in a special spectroelectrochemical cell. The details of the cell are given elsewhere.[24]

The *in situ* X-ray absorption experiments were performed at the National Synchrotron Light Source (NSLS) at Brookhaven National Laboratory using the beam line X11 A, operating at 2.5 GeV and a typical current of 310 mA. The details pertaining to the design of the monochromator, the resolution, and the detune procedure are given elsewhere.[25] Internal references for energy calibration were used for both vanadium and copper.

Harmonics were rejected by detuning (50%). Data were acquired in transmission mode at the vanadium K-edge and in fluorescence mode at the copper K-edge. XANES spectra were taken every 0.5 eV up to 50 eV after the edge with an integration time of 1 s. EXAFS spectra were collected up to $k = 13$ every 0.05 k with a 3 s integration time.

XAS data analysis.—XANES spectra were normalized to an edge jump of unity. A prior removal of the background absorption was done by subtraction of a linear function extrapolated from the pre-edge region.

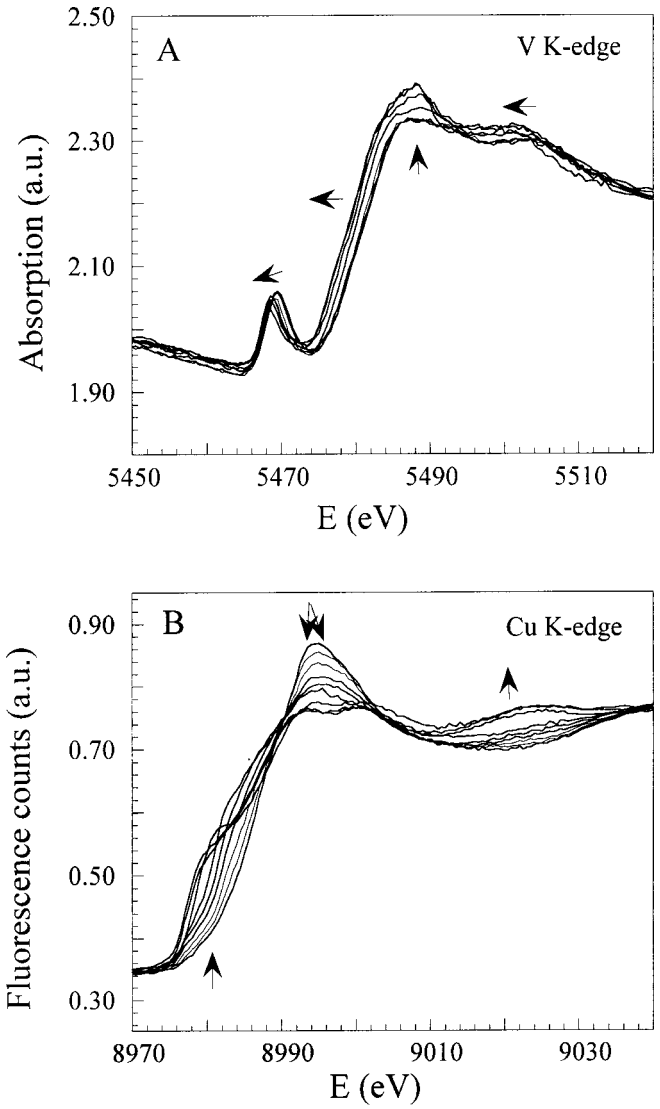

Figure 2. Series of *in situ* XANES spectra of spray-coated $Cu_{0.1}V_2O_5$ electrode as recorded (no background subtracted or normalized) in sequence during discharge (V K-edge, absorption) and charge (Cu K-edge, fluorescence yield).

The EXAFS analysis has been performed by using the GNXAS package[26,27] that takes into account multiple scattering (MS) theory. The method is based on the decomposition of the EXAFS signals into a sum of several contributions, the *n*-body terms. It allows for the direct comparison of the raw experimental data with a model theoretical signal. The procedure avoids any filtering of the data and allows for a statistical analysis of the results. The theoretical signal is calculated *ab initio* and contains the relevant two-body $\gamma^{(2)}$ and the three-body $\gamma^{(3)}$ multiple scattering (MS) terms. The two-body terms are associated with pairs of atoms and probe their distances and variances. The three-body terms allow distances and angles to be probed. If useful, a single effective MS signal $\eta^{(3)}$ that includes both $\gamma^{(2)}$ and the $\gamma^{(3)}$ contributions can be used for the shells beyond the second one by using the same three-atom coordinates both for the two-atom and the three-atom combinations. Phase shifts for the photoabsorber and backscatterer atoms were calculated according to the muffin-tin approximation. The Hedin-Lundvquist complex potential[28] was used for the exchange-correlation potential of the excited state. The core hole lifetime, Γ_c, was kept fixed to the tabulated value[29] and was included in the phase shift calculation.

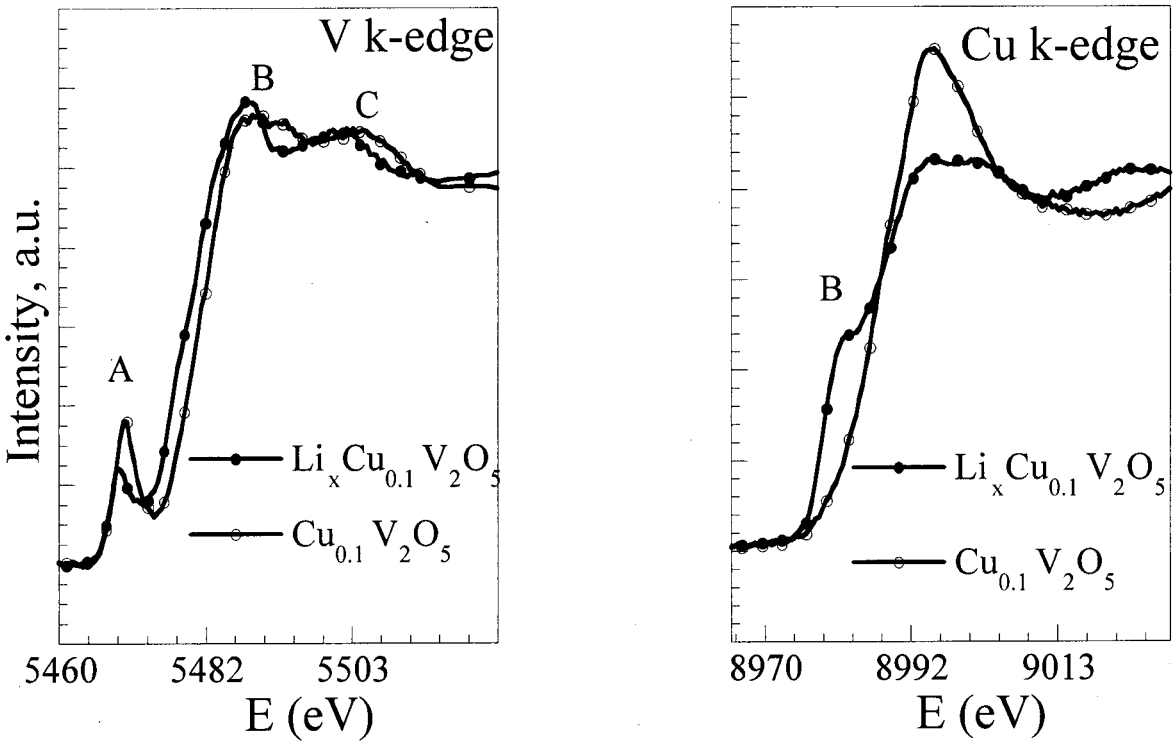

Figure 3. Normalized XANES spectra of pristine and lithiated ($x = 1.5$) $Cu_{0.1}V_2O_5$ XRG cathode (fluorescence mode) taken at the V and Cu K-edge. The V K-edge was recorded during the cathodic scan, the Cu K-edge during the subsequent anodic scan.

The experimental resolution used in the fitting analysis was about 2 eV, in agreement with the stated value for the beamline used. In order to evaluate the effect of the structural disorder, the simulation was done by considering a non-Gaussian type of pair distribution functions. In fact, because of the amorphous nature of the compound, a more flexible model that replaces the simple Gaussian function might be expected to be required. The gamma-like (Γ) distribution has been used here[30,31] and proved to be very useful in previous studies systems.[32,33] The full definition of the function is described in Ref. 30 and 31.

Results and Discussion

Copper-doped V_2O_5 cathodes have excellent properties in terms of electronic conductivity and high intercalation rate.[9,10] Typical discharge performance of a spray-coated $Cu_{0.1}V_2O_5$ electrode as a function of the discharge current is shown in Fig. 1. The material is able to reversibly intercalate more than 2 equiv Li in about 22 h. Even at a very high insertion rate (1.65 mA cm^{-2}) more than 1 equiv Li/mol of active material is intercalated. This result is exceptional, considering that the complete intercalation process takes slightly more than 15 min. In addition, the material shows very good reversibility of the lithium insertion-release process with no capacity fading after more than 450 cycles.[9,10] There is also no loss of Cu to the electrolyte after the 450 cycles.

In situ XAS measurements of the $Cu_{0.1}V_2O_5$ xerogel were performed to investigate the lithium insertion mechanism and the structural modifications that occur in the material upon lithium insertion. The lithium insertion into the electrode was driven by applying a constant current of 0.2 mA for 40 h. The total amount of lithium inserted was 1.5 equiv/mol $Cu_{0.1}V_2O_5$, which corresponds to a delivered capacity of about 200 mAh/g. Two series of XANES spectra were taken at the V and Cu K-edges, respectively, during the lithium insertion. Figure 2A and B shows the raw data at the V and Cu K-edges, respectively. The evolution of the spectra upon increasing the amount of inserted lithium is indicated by the arrows. However, the background profile, due to both ''atomic'' absorption and to the absorption by the electrochemical cell, is rather similar for the entire sequence of XAS curves for a single cell. This similarity indicates there were no secondary processes (such as dissolution of cathodic material nor electrolyte leakage) during the electrochemical cycles. The stable background also indicates that the changes of XAS features accompanying lithium insertion are only due to structural modifications and not to experimental artifacts. In addition, a few isosbestic points[11,16] are shown in the XAS sequences, demonstrating the progressive conversion of the copper species in the pristine $Cu_{0.1}V_2O_5$ to a different copper state in the lithiated compound, and hence the intermediate spectra are a linear combination of the two copper species. They appear at about 5492 and 5503 eV in the V K-edge spectra and at about 8990, 9002, and 9036 eV in the Cu K-edge spectra.

In order to better evaluate the evolution of the XANES features upon lithium insertion, the XANES spectra of the pristine ($Li/V_2=0$) and the lithium-intercalated ($Li/V_2=1.5$) compounds were normalized at both vanadium and copper K-edges (Fig. 3). The normalized spectra show modifications of the V and Cu atoms upon lithium insertion. In particular, the charge (and thus the effective oxidation state) of both vanadium and copper decreased, as indicated by the relative shift toward lower energy of the pre-edge feature in the V K-edge (peak A) and of the peak B in the Cu K-edge. Peak A in the V K-edge spectrum is due to a formally forbidden 1s-3d electronic transition[21,34] that becomes allowed when there is a distortion of the local symmetry. Peak B in the Cu K-edge spectrum is a well-studied fingerprint and it has been assigned to the 1s-4p + shakedown transition.[35,36] Because the photoelectron final state is in both cases related to bound states, the two peaks provide a good indication of the formal oxidation state of the two species (V and Cu). We conclude that the negative charge provided during the reduction process goes onto both metal sites.

Other modifications induced in the XANES spectra by the lithium insertion are ascribed to structural changes of the environ-

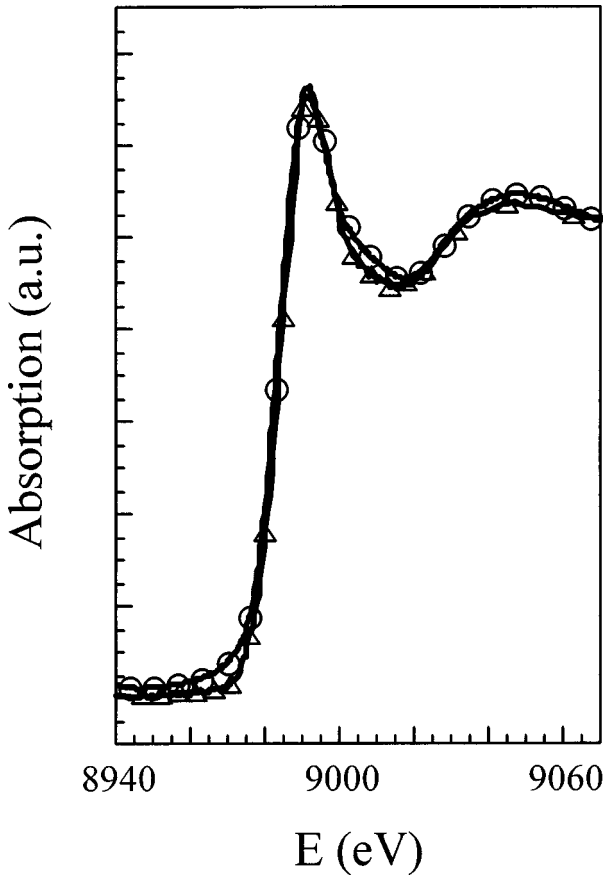

Figure 4. Comparison of the XANES curves (Cu K-edge) for $Cu_{0.1}V_2O_5$ XRG: (○) pristine and (△) after one discharge-charge cycle.

ment of the metals. In the case of vanadium, the modification of the XANES curve shape fully agrees with a previous XAS characterization of electrochemically lithiated xerogels.[21] The position of the feature B, that is called edge resonance, moves toward lower energy. Also, feature B changes shape from two well-defined peaks to a single one. Feature C gives information about the first-shell atoms surrounding the vanadium[21] and moves to lower energy as well. Overall, the XANES spectrum of the native $Cu_{0.1}V_2O_5$ at the V K-edge is rather similar to that of $Zn_{0.14}V_2O_5$.[18] On the other hand, the copper environment undergoes a very interesting modification upon lithiation of the cathode material. The chemical shift of the XANES curves indicated a sharp reduction of the oxidation state of copper. In addition, a close inspection of the shape of the $Li_{1.5}Cu_{0.1}V_2O_5$ curve shows a close similarity to the XANES spectrum of pure Cu.[37] Both pieces of evidence point to the formation of metallic copper upon lithiation. Even more interesting, the modification taking place on the copper atoms is fully reversible as indicated by the full reversibility of the XANES spectrum after full delithiation of the material (see Fig. 4). This verifies the reversibility of the electrochemical process and validates the experimental approach.[21,24,25]

In order to verify this hypothesis, we have analyzed EXAFS spectra recorded during the electrochemical insertion and release processes. Figure 5 shows the EXAFS spectra of pristine and lithiated $Cu_{0.1}V_2O_5$ xerogel and the corresponding Fourier transform (FT). From the extracted EXAFS signals shown in the left frame, it is clear that the local structure around Cu changes dramatically. It is worth noting that the maximum moves toward higher k values, indicating a dramatic change in the backscatterer atomic number from light to heavy atom. This could be made possible, for instance, by a first shell change from Cu-O to a Cu-Cu. In fact, it appears that there is a possible Cu-Cu or Cu-V dominant interaction in the spectrum of $Li_{1.5}Cu_{0.1}V_2O_5$. The relative FT in the right panel is characterized by a shift of the main peak from 1.6 to 2.2 Å and shows contributions up to about 4 Å. In addition, the reduction of Cu^{2+} ion to Cu_2O can be excluded because the latter compound would have a Cu-O first shell at about 1.84 Å.[37]

In order to definitively determine the structure surrounding the copper site in the lithiated cathode, we considered different structural models, which involve the above-mentioned Cu-Cu, Cu-V first-shell interactions, and a possible Cu-O interaction where the oxygen belongs to the host structure. Then we compared it with the experimental EXAFS spectrum of the $Li_{1.5}Cu_{0.1}V_2O_5$. The fit outcome indicates that the signal originating from the Cu-Cu interaction was the only one showing an amplitude shape comparable to the experimental spectrum. Therefore, the structural model for the reduced state was chosen to be that of copper metal.

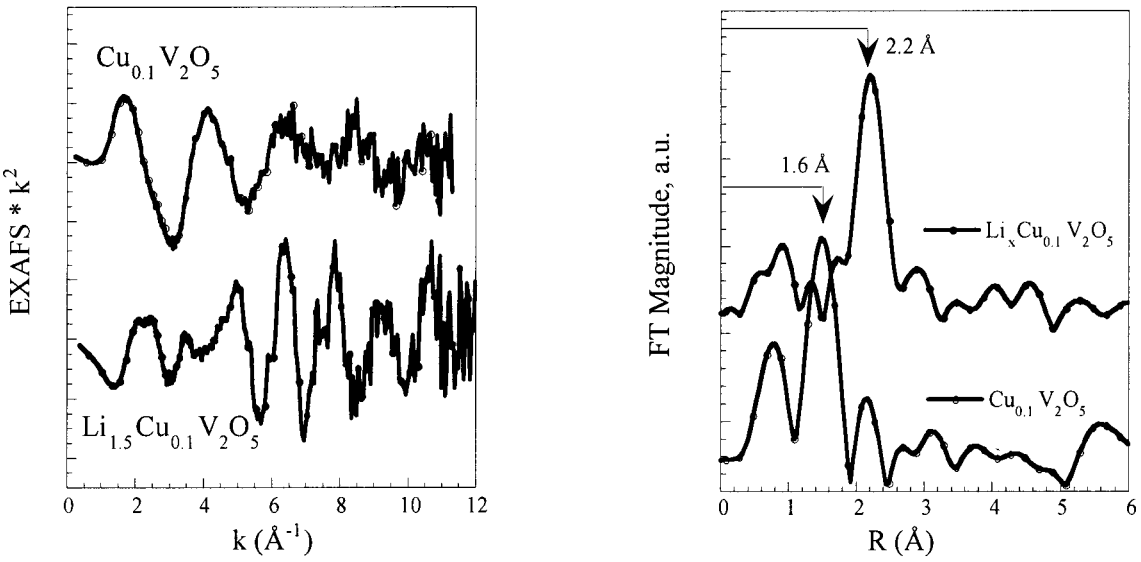

Figure 5. K^2-weighted EXAFS and corresponding FT curve at the copper K-edge of pristine and lithiated ($x = 1.5$) $Cu_{0.1}V_2O_5$ XRG cathode, spectra taken *in situ* and in fluorescence mode. FT conditions: Δk = 3.4-13.5, k^2 weighted.

Table I. Atomic distances and bond lengths of copper metal as seen from the copper atom.

Two body	Distance (Å)	Number of atoms (Degeneracy)	Type
1	2.556	12	Cu
2	3.615	6	Cu
3	4.427	24	Cu
4	5.112	12	Cu

Three body	r1 (Å)	r2 (Å)	Theta (°)	Degeneracy	Types	Half-distance (Å)
1	2.556	2.556	60	24	Cu-Cu-Cu	3.834
2	2.556	2.556	90	36	Cu-Cu-Cu	4.363
3	2.556	2.556	120	72	Cu-Cu-Cu	4.769
4	2.556	2.556	180	18	Cu-Cu-Cu	2.112

With the MS formalism, the atomic arrangement around the copper atom is described by a few important contributions. Table I indicates the most relevant two- and three-body contributions of metallic copper reported in the literature.[37] All the two-body contributions were included in the fitting procedure and only the three-body contribution, noted no. 4 in Table I, was included. The reason for this choice resides in the presence of a 180° angle in that atomic configuration that generates the ''focusing effect'' [38,39] and in turn a signal of non-negligible intensity. Refining the calculations and taking Table I as reference, the following two-atom contributions, $\lambda_1^{(2)}$ Cu-Cu with degeneracy of 12, $\gamma_1^{(2)}$ Cu-Cu with degeneracy of 6, $\gamma_3^{(2)}$ Cu-Cu with degeneracy of 24, corresponding to the first, second and third shell, respectively, and the three-atom contribution, *i.e.*, the Cu-Cu-Cu triplet term $\gamma_4^{(3)}$, where the $\eta_4^{(3)}$ notation includes both $\gamma_4^{(3)}$ Cu-Cu-Cu (degeneracy of 18) and $\gamma_4^{(2)}$ Cu-Cu (degeneracy of 12), were included in the fitting procedure. The overall number of structural parameters included in the fitting procedure was eight.

The results of the fit are illustrated in Fig. 6. The figure shows the theoretical contribution of each MS contribution (upper curves) and the comparison of the total theoretical signal $k\chi(k)$ with the experimental one (bottom curve). From the lower plot it is seen that the theoretical curve matches well with the experimental one. In addition, it is clearly seen that although the first-shell contribution dominates the total signal (signal $\gamma_1^{(2)}$ Cu-Cu), the inclusion of the other signals was needed to account for the high-frequency pattern of the EXAFS $\chi(k)$ spectra.

The interatomic distances, and the corresponding EXAFS Debye-Waller factors of the $Li_{1.5}Cu_{0.1}V_2O_5$ obtained from the best fit, are shown in Table II. The nonstructural parameters E_0 and S_0^2 have been found to be 8984(4) eV and 0.88(5), respectively. The errors associated with the parameters obtained with the EXAFS analysis are indicated as well. The latter were determined by correlation maps (contour plots) for each pair of parameters. Figure 7 shows the contour plot for the Cu-Cu first shell and the highly correlated E_0 variable. The estimated statistical error is associated with a 95% confidence interval.[40]

The results of the present work, reported in Table II, agree with literature data on metallic copper (Table I). This certainly means that the copper environment in lithiated copper-doped V_2O_5 XRG ($Li_{1.5}Cu_{0.1}V_2O_5$) is close to that of Cu metal. However, the growth of metallic copper clusters upon lithiation is strongly constrained by the internal structure of the host, *i.e.*, the V_2O_5 bilayered structure.[21] This also causes structural disorder, as evidenced by the use of a non-Gaussian model for the bond length distribution. The particular configuration of the copper atoms is indicated by the actual coordination number (CN) obtained from the fit of the experimental data. In fact, the best fit was obtained by multiplying the multiplicity of

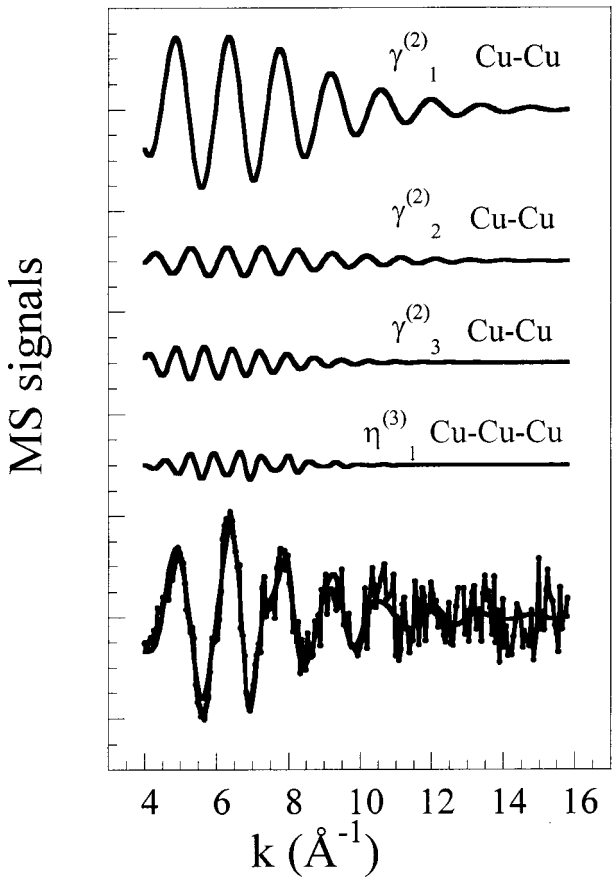

Figure 6. Interpretation and fit analysis of the Cu K-edge EXAFS spectrum recorded of the lithiated ($x = 1.5$) $Cu_{0.1}V_2O_5$ XRG cathode. The plot shows the various contributions to the total theoretical signal, and shows a comparison between the theoretical and the experimental ones.

Table II. EXAFS best-fitting results. The estimated parameter errors are indicated in parentheses.

	1st shell Cu-Cu	2nd shell Cu-Cu	3rd shell Cu-Cu	Cu-Cu-Cu angle
Distance (Å)	2.54 (2)	3.57 (4)	4.44 (4)	180[a]
$\sigma^2/(Å^2)$	0.008(3)	0.008(4)	0.017(10)	60[b]
CN[c]	4	2	8	

[a] The angle was kept fixed at the crystallographic value.
[b] Angle variance in deg^2.
[c] CN as it appears in Table I and considering the multiplicity factor 0.34 from the fitting procedure.

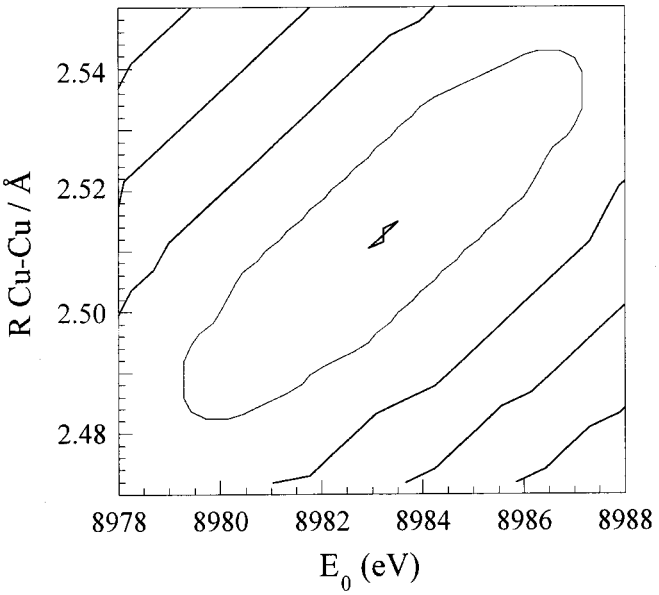

Figure 7. Two-dimensional section of the parameter space referring to the R Cu-Cu (first shell) and E_0. The inner elliptical contour corresponds to the 95% confidence level.

each MS contribution by a factor of 0.34.[10] Taking account of this factor, the number of first-neighbors of Cu in lithiated $Cu_{0.1}V_2O_5$ is (12×0.34), *i.e.*, about 4. The relative CNs for the other shells are reported in Table II. The amplitude reduction observed in the EXAFS spectra could be interpreted as due to the existence of a large density of structural defects in the metallic copper in the lithiated material. Therefore, our experimental findings are explained on the basis of a simple model which takes into account the presence of atomic defects and vacancies that lead to marked reduction of the coordination numbers and of the three-atom multiplicities.[41]

In the $Li_{1.5}Cu_{0.1}V_2O_5$, the copper aggregates as small domains of metal that are sandwiched between the bilayers of V_2O_5.

Conclusions

The present work has characterized the modification of the structure taking place in copper-doped V_2O_5 XRG upon lithium insertion. Cathodes of such a material have shown excellent electrochemical properties in terms of lithium insertion capacity both in the form of aerogels and xerogels. The materials reversibly insert up to 2.2 mol Li per mole of doped V_2O_5 over a few hundred cycles (>450) with no capacity fading.

The work was based on the use of a synchrotron radiation source to acquire *in situ* XAS spectra. The experiments were performed at the National Synchrotron Light Source, Brookhaven National Laboratory, an experimental setup which allowed real-time data recording. Data analysis was performed by using the MS formalism (GNXAS).

The results have shown that the lithium insertion in copper-doped V_2O_5 XRG causes reduction of both copper and vanadium atoms. While the vanadium site is modified by lithium insertion as in other XRGs, the copper ions are reduced to the metallic state. Under the constraint of the bilayered structure of the host, the metallic copper domains have many defects and atomic vacancies. This conclusion confirms the electrochemical result that showed metallic copper formation reported previously for Cu- and Ag-doped V_2O_5 XRGs. In that previous work, the formation of metallic copper (or silver) was indicated as the cause of the excellent lithium insertion performance of the doped materials, which was caused by the increase of electronic conductivity upon lithiation. Of further importance, the present work has shown that the process is completely reversible at the atomic level.

In order to understand the role of Cu in the native cathode ($Cu_{0.1}V_2O_5$), an exhaustive XAFS analysis on solid-state samples is in progress and will be presented in a forthcoming paper.[42]

Acknowledgment

We appreciate the support of DOE under contract DE-FG02-93ER14384.

The University of Minnesota assisted in meeting the publication costs of this article.

References

1. J. Livage, *Coord. Chem. Rev.*, **178-180**, 999 (1998).
2. T. Chirayil, P. Y. Zavalij, and M. S. Whittingham, *Chem. Mater.*, **10**, 2629 (1998).
3. D. B. Le, S. Passerini, A. L. Tipton, B. B. Owens, and W. H. Smyrl, *J. Electrochem. Soc.*, **142**, L102 (1995).
4. F. Coustier, S. Passerini, and W. H. Smyrl, *J. Electrochem. Soc.*, **145**, L73 (1998).
5. D. B. Le, S. Passerini, J. Guo, J. Ressler, B. B. Owens, and W. H. Smyrl, *J. Electrochem. Soc.*, **143**, 2099 (1996).
6. P. P. Prosini, S. Passerini, R. Vellone, and W. H. Smyrl, *J. Power Sources*, **75**, 73 (1998).
7. D. B. Le, S. Passerini, F. Coustier, J. Guo, T. Soderstrom, B. B. Owens, and W. H. Smyrl, *Chem. Mater.*, **10**, 682 (1998).
8. F. Coustier, J-M. Le, S. Passerini, and W. H. Smyrl, *Solid State Ionics*, **116**, 279 (1999).
9. F. Coustier, J. Hill, B. B. Owens, S. Passerini, and W. H. Smyrl, *J. Electrochem. Soc.*, **146**, 1355 (1999).
10. F. Coustier, G. Jarero, S. Passerini, and W. H. Smyrl, *J. Power Sources*, **83**, 9 (1999).
11. H. D. Abruna, *Electrochemical Interfaces: Modern Techniques for In-Situ Interface Characterization*, p. 1-556, VCH, New York (1991).
12. L. Blum, H. D. Abruna, J. H. White, J. G. Gordon, G. L. Borges, M. G. Samant, and O. R. Melroy, *J. Chem. Phys.*, **85**, 6732 (1986).
13. A. Tadjeddine, D. Guay, M. Ladouceur, and G. Tourillon, *Phys. Rev. Lett.*, **66**, 2335 (1991).
14. P. G. Allen, S. D. Conradson, and J. E. Penner-Hahn, *Synchrotron Radiat. News*, **5**, 16 (1992).
15. J. McBreen, S. Mukerjee, and X. Q. Yang, *Synchrotron Radiat. News*, **11**, 18 (1998).
16. M. Giorgetti, I. Ascone, M. Berrettoni, P. Conti, S. Zamponi, and R. Marassi, *J. Biol. Inorg. Chem.*, **5**, 156 (2000).
17. S. Passerini, D. B. Le, W. H. Smyrl, M. Berrettoni, R. Tossici, R. Marassi, and M. Giorgetti, *Solid State Ionics*, **104**, 195 (1997).
18. M. Giorgetti, S. Passerini, W. H. Smyrl, and M. Berrettoni, *Chem. Mater.*, **11**, 2257 (1999).
19. M. Giorgetti, S. Passerini, M. Berrettoni, and W. H. Smyrl, *J. Synchrotron Radiat.*, **6**, 743 (1999).
20. M. Giorgetti, M. Berrettoni, S. Passerini, and W. H. Smyrl, in *Lithium Batteries*, S. Surampudi and R. A. March, Editors, PV 98-16, p. 356, The Electrochemical Society Proceedings Series, Pennington, NJ (1999).
21. M. Giorgetti, S. Passerini, W. H. Smyrl, S. Muckerjee, X. Q. Yang, and J. McBreen, *J. Electrochem. Soc.*, **146**, 2387 (1999).
22. M. Giorgetti, S. Passerini, W. H. Smyrl, and M. Berrettoni, *Inorg. Chem.*, **39**, 1514 (2000).
23. M. Giorgetti, S. Passerini, and W. H. Smyrl, Abstract 125, The Electrochemical Society and The Electrochemical Society of Japan Meeting Abstracts, Vol. 99-2, Honolulu, HI, Oct 17-22, 1999.
24. J. McBreen, S. Mukerjee, X. Q. Yang, T. R. Thurston, and N. M. Jisrawi, in *Second International Symposium on New Materials for Fuel Cells and Modern Battery Systems*, O. Savadogo and P. R. Roberge, Editors, p. 348 (1997).
25. J. McBreen and S. Mukerjee, *J. Electrochem. Soc.*, **142**, 3399 (1995).
26. A. Filipponi, A. Di Cicco, and C. R. Natoli, *Phys. Rev. B*, **52**, 15122 (1995).
27. A. Filipponi and A. Di Cicco, *Phys. Rev. B*, **52**, 15135 (1995).
28. L. Hedin and B. I. Lundvquist, *J. Phys. C*, **4**, 2064 (1971).
29. M. Krause and J. H. Oliver, *J. Phys. Chem. Ref. Data*, **8**, 329 (1979).
30. A. Filipponi, *J. Phys.: Condens. Matter*, **6**, 8415 (1994).
31. A. Filipponi and A. Di Cicco, *Task Quarterly*, **4**, 575 (2000).
32. P. D'Angelo, A. Di Nola, A. Filipponi, N. V. Pavel, and D. Roccatano, *J. Chem. Phys.*, **100**, 985 (1994).
33. A. Filipponi and A. Di Cicco, *Phys. Rev. B*, **51**, 12322 (1995).
34. J. Wong, F. W. Lytle, R. P. Messmer, and D. H. Maylotte, *Phys. Rev. B*, **30**, 5596 (1984).
35. R. A. Bair and W. A. Goddard III, *Phys. Rev. B*, **22**, 2767 (1980).
36. N. Kosugi, T. Yokoyama, K. Asakura, and H. Kuroda, *Chem. Phys.*, **91**, 249 (1984).
37. R. W. Wyckoff, *Crystal Structures*, Interscience Publishers, New York (1965).

38. A. Filipponi, A. Di Cicco, M. Benfatto, and C. R. Natoli, *Europhys. Lett.*, **13**, 319 (1990).
39. M. Giorgetti, M. Berrettoni, A. Filipponi, P. J. Kulesza, and R. Marassi, *Chem. Phys. Lett.*, **275**, 108 (1997).
40. A. Filipponi, *J. Phys.: Condens. Matter*, **7**, 9343 (1995).
41. A. Di Cicco, M. Berrettoni, S. Stizza, E. Sonetti, and G. Cocco, *Phys. Rev. B*, **50**, 12386 (1994).
42. M. Giorgetti *et al.*, In preparation.